INORGANIC CHEMISTRY FRONTIERS

RESEARCH ARTICLE

View Article Online
View Journal | View Issue

Cite this: *Inorg. Chem. Front.*, 2023, **10**, 7285

Acid-induced conversion of nitrite to nitric oxide at the copper(II) center: a new catalytic pathway†

Prabhakar Bhardwaj,[a] Kulbir,[a] Tarali Devi*[b] and Pankaj Kumar*[a]

Acid-induced reduction of nitrites (NO_2^-) to nitric oxide (NO) at Cu/Fe centers is one of the key steps in the nitrogen cycle and serves as an essential path to NO generation. In this study, we report the acid-catalysed conversion of NO_2^- to NO at the Cu^{II} centers in Cu^{II}-nitrito complexes, $[(Me_2BPMEN)Cu^{II}(NO_2^-)]^+$ (**1**) and $[(H_2BPMEN)Cu^{II}(NO_2^-)]^+$ (**2**). Both the Cu^{II}-NO_2^- complexes showed the formation of $NO_{(g)}$ along with H_2O_2 when reacted with one equivalent acid (H^+) *via* the N–O bond homolysis of the presumed Cu^{II}-nitrous acid ($[Cu\text{-}ONOH]^{2+}$) intermediate. However, the H_2O_2 amount decreased with time or an increase in H^+ and completely disappeared when H^+ was more than about two equivalents accompanied by the generation of H_2O. We detected the released $NO_{(g)}$ by using headspace gas chromatography/mass spectrometry; moreover, the $NO_{(g)}$ evolution was confirmed by the formation of a significant amount of $\{CoNO\}^8$, $[(12\text{-}TMC)Co(NO)]^{2+}$ up to (90 ± 5%) in the above reactions. Mechanistic investigations using ^{15}N-labeled-$^{15}NO_2^-$ and ^{18}O-labeled-$^{16}O^{14}N^{18}O^-$ revealed that the N-atom in NO is derived from the $^{18}ONO^-$ ligand, which was further confirmed by the detection of ^{15}NO and $N^{18}O$ gas in headspace gas chromatography/mass spectrometry. We also monitored and characterized the formation of H_2O_2 (one equivalent of H^+) and H_2O (two equivalents of H^+) and the results describe the rationale behind biological NO_2^- reduction reactions generating NO along with H_2O. We observed more than 90% recovery of (1) after 10 catalytic cycles of $NO_{(g)}$ generation.

Received 1st September 2023,
Accepted 24th October 2023

DOI: 10.1039/d3qi01637d

rsc.li/frontiers-inorganic

Nitric oxide (NO) is a gaseous secondary messenger in animals, plants, fungi, and bacteria. NO plays a significant role in various physiological processes, such as neurotransmission, vascular regulation, platelet disaggregation, and immune response to multiple infections, in mammals.[1] Moreover, NO is involved in different physiological processes in plants, such as plant growth and development, metabolism, aging, defense against pathogens, and biotic and abiotic trauma.[2] It is now well-established that NO inadequacy causes atherosclerosis, diabetic hypertension, and other diseases.[3] In addition to the pathological effect, its oxidized species peroxynitrite (PN, $ONOO^-$)[4] and nitrogen dioxide ($^{\bullet}NO_2$)[5] are known for their immune response towards harmful pathogens; however, they may also lead to various toxicological behaviors.[4b,6] Hence, the balanced production of NO is required to maintain multiple physiological processes (homeostasis). In this regard, NO_2^- reductases (NiRs)[7] and endothelial nitric oxide synthases (eNOSs)[7c,8] are the enzymes available for biological NO generation. The critical substrate of the NOSs system for the generation of NO is L-arginine, which changes to citrulline with the simultaneous release of NO following catalytic activity.[8]

In recent years, a few *in vitro* functional models have been prepared and investigated to obtain mechanistic insights into the NO_2^- reduction chemistry. In this regard, three types of reactions have been explored: (i) H^+-induced NO_2^- reduction (mimicking NiR), (ii) oxygen atom transfer (OAT) triggered by thioether (R_2S)[9]/thiol (RSH)[10]/triphenylphosphine (PPh_3),[11] and (iii) the photo-induced reactions[12] of metal-bound NO_2^- ($M\text{-}NO_2^-$) species. Karlin and co-workers developed a heme-Fe/Cu assembly model to mimic cytochrome c oxidase, illustrating the reversible conversion of NO_2^- to NO.[13] In 1937, Brooks first proposed the NiR activity of hemoglobin upon its reaction with NO_2^- and observed the formation of NO and metHb in anaerobic conditions.[14] Recently, chemistries for modeling the M-NOs/active sites associated with NiR and NOS have also been explored.[15] Recently, Lehnert *et al.* developed a synthetic approach for Fe-NOs,[16] and Hayton structurally characterized the first Cu^{II}-NO.[17] Nam and coworkers probed the generation of Fe-NOs by photo-induced NiR reactivity and stabilized the Co-NOs.[18] Chen-Hsiung Hung and co-workers reported H^+-induced Fe^{II}-NO_2^- reduction and the generation of Fe^{III}-NO

[a]*Departzment of Chemistry, Indian Institute of Science Education and Research (IISER), Tirupati 517507, India. E-mail: pankajatiisert@gmail.com, pankaj@iisertirupati.ac.in*
[b]*Department of Inorganic and Physical Chemistry, Indian Institute of Science, Bangalore 560012, India*

†Electronic supplementary information (ESI) available. CCDC 2176961 and 2176962. For ESI and crystallographic data in CIF or other electronic format see DOI: https://doi.org/10.1039/d3qi01637d

with H_2O.[19] Ford and coworkers described NiR chemistries in Fe-heme systems and characterized Fe-NOs formation.[20] Although NiR plays an essential part in NO generation, it has not been investigated extensively to identify the end products and understand the reaction mechanism.

In addition to biomimetic modeling of the NiR enzyme, a few reports on NO_2^- reduction to NO have also been explored to understand the reaction mechanism of stabilizing the metal-nitrosyls or efficiently generating NO. Elizabeth T. Papish and coworkers showed NO release with H_2O *via* a Cu^I-NO^+ ↔ Cu^{II}-NO intermediate in the reaction of Cu^{II}-NO_2^- with two equivalents of H^+.[21] Murphy *et al.*, for the first time, explained the generation of NO *via* a Cu-NO intermediate species in a Cu-NO_2^- reduction reaction along with the structural details of the Cu-NO complex.[7b] Ford and coworkers reported the NO_2^- reduction reaction of Fe-porphyrin catalysed by R_2S and tetrahydrothiophene.[9] Todd C. Harrop and coworkers described a non-heme Fe^{II}-$(NO_2^-)_2$ complex that undergoes a catalytic NO_2^- reduction reaction in the presence of RSH and H^+.[10a] A study on the Cu-NO_2^- complex conducted by Warren *et al.*, using thiol as the reducing agent gives a brief direction about the mechanism of O-atom transfer.[10b] Sodio C. N. Hsu *et al.* showed NO release along with H_2O in the reaction of Cu^I-NO_2^- with two equivalents of acetic acid.[22] Patra *et al.* showed the generation of NO + H_2O in the Cu^{II}-NO_2^- + $2H^+$ reaction.[23] Hunt *et al.* showed NO generation through the electrolytic reduction of NO_2^- at the copper center. Lenhert and Coworker explored a new O_2-tolerant Cu^{II}-complex-based catalyst that electrochemically reduces NO_2^- to NO at the optimal potential.[24] Recently, for the very first time, we have demonstrated the H^+-induced reduction of Co^{II}-NO_2^- to {CoNO}[8] with H_2O_2 generation;[25] and in another case, the generation of {FeNO}[7] and H_2O from Fe^{II}-NO_2^- *via* the H_2O_2 intermediate in the presence of H^+.[26]

Recent studies on H^+-induced NO_2^- reduction have shown the generation of NO with different by-products (H_2O, H_2O_2 and NO_2), while they were not found/explored for the catalytic conversion mechanism of NO_2^- to $NO_{(g)}$.[26,27] Therefore, we need to explore these reactions to understand the basis for the formation of different side products in the H^+-induced conversion of NO_2^- to $NO_{(g)}$ and to develop a suitable catalyst for selective catalytic $NO_{(g)}$ generation under optimum conditions. Minimal work has been done on H^+-induced catalytic $NO_{(g)}$ generation from metal-NO_2^- species; however, there are a few reports on electrocatalytic NO formation from metal-NO_2^-.[24,28] Being a very important biological molecule (*vide supra*), developing a catalyst for selective $NO_{(g)}$ formation *via* H^+-induced NO_2^- transformation is highly necessary to treating several biological dysfunctions. In the last few years, we have successfully developed a few models for NO_2^- reduction to NO on cobalt and iron centers, demonstrating metal-nitrosyls formation.[26,29] Hence, here, we intend to develop a suitable molecular catalyst for catalytic $NO_{(g)}$ generation and to understand the reaction mechanism of H^+-induced NO_2^- disproportionation toward $NO_{(g)}$ formation at the Cu^{II}-centers in Cu^{II}-NO_2^- complexes.

We, herein, report the synthesis of $NO_{(g)}$ *via* H^+-induced NO_2^- transformation in two different Cu^{II}-NO_2^- complexes, namely $[(Me_2BPMEN)Cu^{II}(NO_2^-)]^+$ (**1**) and $[(H_2BPMEN)Cu^{II}(NO_2^-)]^+$ (**2**), which bear the *N*,*N*′-dimethyl-*N*,*N*′-bis(2-pyridylmethyl)-1,2-diaminoethane (Me_2BPMEN) and *N*,*N*′-bis(2-pyridylmethyl)-1,2-diaminoethane (H_2BPMEN) ligands, respectively (Scheme 1). Complex **1** reacted with one equivalent perchloric acid ($HClO_4$, H^+ source) and generated NO gas ($NO_{(g)}$) with $[(Me_2BPMEN)Cu^{II}]^{2+}$ (**3**) and H_2O_2 *via* the formation of a presumed Cu^{II}-nitrous acid intermediate ([Cu-ONOH]$^{2+}$) in CH_3CN at 298 K (Scheme 1, reactions II and III). However, an increase in the H^+ equivalent showed a significant fall in the H_2O_2 amount. It disappeared completely when the H^+ quantity crossed two/more equivalents along with the simultaneous formation of a substantial amount of H_2O (Scheme 1, reaction IV). Similarly, an equimolar amount of H^+ could convert NO_2^- to $NO_{(g)}$ accompanied by H_2O_2 formation on complex **2** (Scheme 1, reactions II and III); however, upon its reaction with excess H^+ (~two or more equiv.), we observed the generation of $NO_{(g)}$ and H_2O (Scheme 1, reaction IV). Meanwhile, the initial Cu^{II}-complexes (**3**/or **4**) were found to be unreactive towards NO, suggesting that the formation of {CuNO}[10] species is not possible from these complexes (Scheme 1, reaction V). Mechanistic investigations using ^{15}N-labeled-$^{15}NO_2^-$ demonstrated explicitly that the N-atom in the evolved $NO_{(g)}$ is derived from the NO_2^- anion, and H_2O_2 comes from ON–OH bond homolysis. Further exploration of NO_2^- to $NO_{(g)}$ conversion in the presence of excess H^+ ions showed H_2O formation *via* H^+-induced H_2O_2 decomposition in addition to $NO_{(g)}$ evolution.[30] To our knowledge, this work reports a new mechanism, showing that the H^+-induced NO_2^- disproportionation/conversion reaction on Cu^{II} centers indeed generates $NO_{(g)}$ and H_2O as the end products *via* the proposed $[M^{n+}$-ONOH$]^{n+}$ intermediate. However, the H_2O molecule is believed to be formed either by the auto-decomposition (H^+ = one equiv.)[31] or H^+-induced conversion (H^+ = two or more equiv.)[30,32] of the H_2O_2 intermediate species produced from the homolysis of the ON–OH moiety.[25] The new findings indicate that NO_2^- converts to $NO_{(g)}$ *via* the homolysis of the NO–OH moiety and that H_2O formation *via* the decomposition of the H_2O_2 intermediate species depends on the H^+ concen-

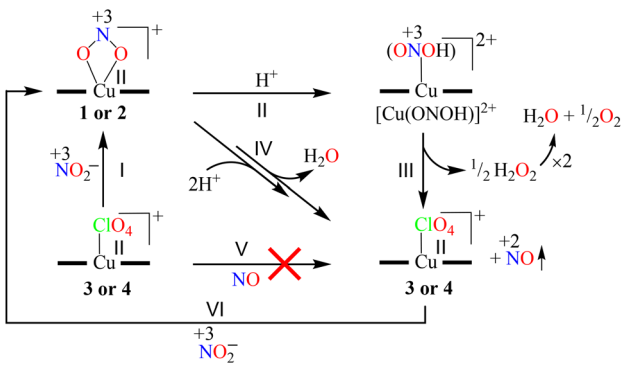

Scheme 1

tration. These results add new insights not only to the previously explored *in vitro* NO_2^- reduction chemistry[33] but also to other reported chemistries on NO_2^- to $NO_{(g)}$ transformation.[34]

Results and discussion

Synthesis of the Cu^{II}-nitrite (Cu^{II}-NO_2^-) complexes $[(Me_2BPMEN)Cu^{II}(NO_2^-)]^+$ (1) and $[(H_2BPMEN)Cu^{II}(NO_2^-)]^+$ (2)

The initial Cu^{II}-NO_2^- complexes, **1** and **2**, were prepared by the addition of one equivalent of $NaNO_2$ to the Cu^{II} complexes $[(Me_2BPMEN)Cu^{II}]^{2+}$ (**3**) and $[(H_2BPMEN)Cu^{II}]^{2+}$ (**4**),[35] respectively, in CH_3CN at 298 K (Scheme 1, reaction I; also see ESI† and Experimental section (ES)). Complexes **1** and **2** were characterized by various spectroscopic measurements, including the single-crystal X-ray structure determination of **1**.[18a,b] In the UV-vis spectra, the addition of one equivalent of $NaNO_2$ to **3** led to the formation of a new band at (λ_{max} = 375 nm) in CH_3CN at 298 K, which corresponds to **1** (Fig. 1a; ESI, Fig. S1a†). The FT-IR spectrum of **1** showed a characteristic peak at 1270 cm^{-1}, which shifted to 1244 cm^{-1} and 1243 cm^{-1} when exchanged with ^{15}N-labeled-nitrite (**1**-$^{15}N^{16}O_2^-$) and ^{18}O-labeled-nitrite (**1**-$^{18}ONO^-$) (inset, Fig. 1a; ESI, Fig. S1b–d†). The electrospray ionization mass spectra (ESI-MS) recorded for **1** showed a prominent ion peak at *m*/*z* 379.1, which shifted to *m*/*z* 380.1 when prepared with ^{15}N-labeled $Na^{15}N^{16}O_2$; their mass and isotope distribution pattern corresponded with $[(Me_2BPMEN)Cu^{II}(NO_2^-)]^+$ (calc. *m*/*z* 379.1) and $[(Me_2BPMEN)Cu^{II}(^{15}NO_2^-)]^+$ (calc. *m*/*z* 380.1), respectively (Fig. 1b; ESI, Fig. S1e†). Similarly, the addition of one equivalent of $NaNO_2$ to $[(H_2BPMEN)Cu^{II}]^{2+}$ led to the formation of a new band at (λ_{max} = 360 nm) corresponding to **2** (Fig. 1c; ESI, Fig. S2a†). The FT-IR spectrum of **2** showed a characteristics peak at 1270 cm^{-1}, which shifted to 1244 cm^{-1} when exchanged with ^{15}N-labeled-nitrite (**2**-$^{15}N^{16}O_2^-$) (inset, Fig. 1c; ESI, Fig. S2b and c†). The electrospray ionization mass spectra (ESI-MS) recorded for **2** showed a prominent ion peak at *m*/*z* 351.1, which shifted to *m*/*z* 352.1 when prepared with ^{15}N-labeled $Na^{15}N^{16}O_2$; their mass and isotope distribution pattern corresponded with $[(H_2BPMEN)Cu^{II}(NO_2^-)]^+$ (calc. *m*/*z* 351.1) and $[(H_2BPMEN)Cu^{II}(^{15}NO_2^-)]^+$ (calc. *m*/*z* 352.1), respectively (Fig. 1d; ESI, Fig. S2d†). Moreover, **1** was structurally characterized *via* single-crystal X-ray crystallography; however, after several attempts, we failed to get the structure for **2**. The results show that Complex **1** possesses a six-coordinate distorted octahedral geometry around the Cu^{II}-center and contains the O,O′-chelated bi-dentate NO_2^- anion (Fig. 2a; ESI Fig. S3†).[36]

The reaction of $[(Me_2BPMEN)Cu^{II}(NO_2^-)]^+$ (1) with acid

To further investigate the acid (H^+ ions)-catalyzed conversion of NO_2^- to $NO_{(g)}$ at the Cu^{II} center in Cu^{II}-NO_2^- and its mechanistic aspects, we explored the reaction of **1** with different equivalents of H^+. A visible color change from cyan green to deep blue was observed in the reaction of **1** with H^+, and a new absorption band (at 620 nm) was observed in the UV-vis spectral measurements, corresponding to the initial Cu^{II}-complex **3** along with the release of $NO_{(g)}$ in very short

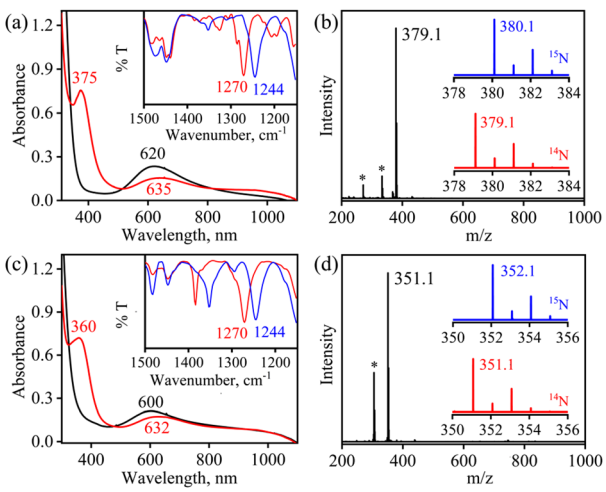

Fig. 1 (a) The UV-vis spectra of **3** (1.0 mM, black line) and **1** (red line). The inset shows the FT-IR spectra of **1**-$^{14}N^{16}O_2^-$ (red line) and **1**-$^{15}N^{16}O_2^-$ (blue line). (b) The ESI-MS spectrum of **1**. The insets show the isotope distribution patterns for **1**-$^{14}N^{16}O_2^-$ (red line) and **1**-$^{15}N^{16}O_2^-$ (blue line). (c) The UV-vis spectra of **4** (1.0 mM, black line) and **2** (red line). The inset shows the FT-IR spectra of **2**-$^{14}N^{16}O_2^-$ (red line) and **2**-$^{15}N^{16}O_2^-$ (blue line). (d) The ESI-MS spectrum of **2**. The insets show the isotope distribution patterns for **2**-$^{14}N^{16}O_2^-$ (red line) and **2**-$^{15}N^{16}O_2^-$ (blue line).

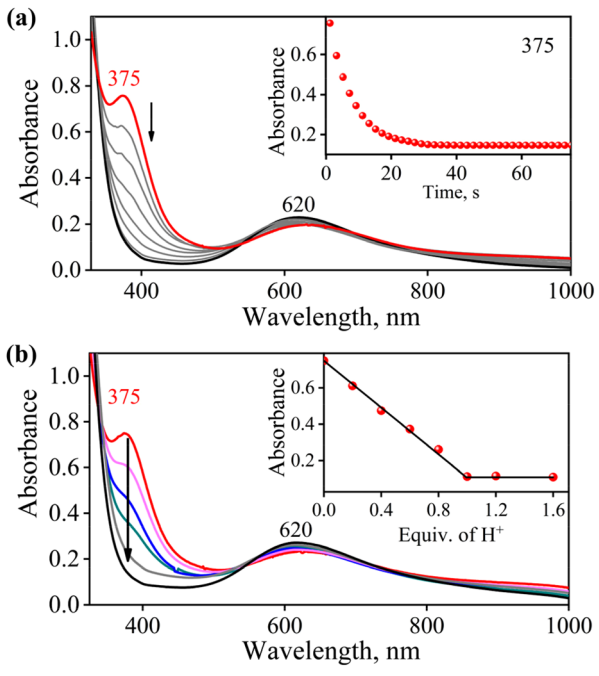

Fig. 2 The displacement ellipsoid plots (50% probability level) of (a) **1** and (b) **3** at 100 K. The H atoms have been omitted for clarity. Gray, C; blue, N; red, O; orange, Cu. The crystallographic data and selected bond lengths (Å) and angles (deg) for **1** and **3** are summarized in Table S1.†

time (Fig. 3a; ES and ESI, Fig. S4†). The ratio-metric equivalent of H^+ with **1** was determined by performing spectral titration and was found to be 1 : 1 (Fig. 3b). The product obtained in the above reaction was confirmed to be **3** based on various spectroscopic measurements (ES, ESI, Fig. S4†) and the single-crystal X-ray structure (Fig. 2b and ESI, Fig. S4e†). Complex **1** was found to be very stable in CH_3CN and at 298 K as it did not show any spectral changes in the absence of H^+ (ES and ESI, Fig. S5†). However, when **1** was reacted with one equivalent of H^+, it generated $NO_{(g)}$ and an equivalent amount of H_2O_2[25] (ESI, Fig. S6†) with **3**, in contrast to the previous reports on NO_2^- reactions that $NO_{(g)}$ is formed along with H_2O molecules.[7b,c,37] The $NO_{(g)}$ released from H^+-catalysed $^{14/15}NO_2^-$ disproportionation on **1** was detected and followed by real-time headspace gas chromatography/mass spectrometric measurements. A high-intensity NO peak was detected upon the addition of one equivalent of H^+ to **1** (Fig. 4a). Further, to track the N atom in the reaction of **1** with one equivalent of H^+, we explored the reaction of **1**-$^{15}NO_2^-$ with one equivalent of H^+, and a major peak for $^{15}NO_{(g)}$ was observed (Fig. 4b). Moreover, carrying out the reaction of **1** with two equivalents of H^+ led to the formation of $^{14/15}NO_{(g)}$, as detected by headspace gas chromatography/mass spectrometry (Fig. 4c and d), which evidently establishes that $^{14/15}NO_{(g)}$ gas was formed in the reaction of **1** with different amounts of H^+. In addition, we observed the formation of $N^{18}O$ and $N^{16}O$ in the reaction of **1**-$^{18}ONO^-$ with one equivalent of H^+, further supporting that $NO_{(g)}$ is indeed formed from the interaction of NO_2^- with H^+ ions at the Cu^{II} center in **1** (Fig. 4e).

It is unique that different amounts of H^+ dictate/regulate the side products of NO_2^- conversion, leading to completely new mechanistic pathways of H^+-induced NO_2^- to $NO_{(g)}$ transformation. The released $NO_{(g)}$ was monitored for qualitative and quantitative estimations in two different ways: (a) trapping it by using $[(12\text{–TMC})Co^{II}(NCCH_3)]^{2+}$, which forms $[(12\text{-TMC})Co(NO)]^{2+}$ ($\{CoNO\}^8$)[25,29,38] and (b) gas-mass spectrometry in CH_3CN under Ar at 298 K (Fig. 4).[7b,c,37] The FT-IR spectrum of $\{CoNO\}^8$, which was formed by the evolved $NO_{(g)}$ + $[(12\text{-TMC})Co^{II}(NCCH_3)]^{2+}$, showed a characteristic peak for Co-bound

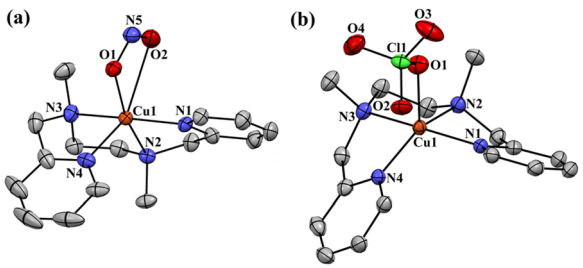

Fig. 3 (a) The UV-vis spectral changes of **1** (1 mM, red line) with the addition of one equivalent of H^+ under Ar in CH_3CN at 298 K. The red spectrum of (**1**) transformed into the black pattern (**3**) upon the addition of one equivalent of H^+. (b) The UV-vis spectral changes observed in the reaction of **1** with incremental H^+ concentrations (0, 0.20, 0.40, 0.60, 0.80, 1.0, 1.2, and 1.6 equivalents) in CH_3CN under Ar at 298 K.

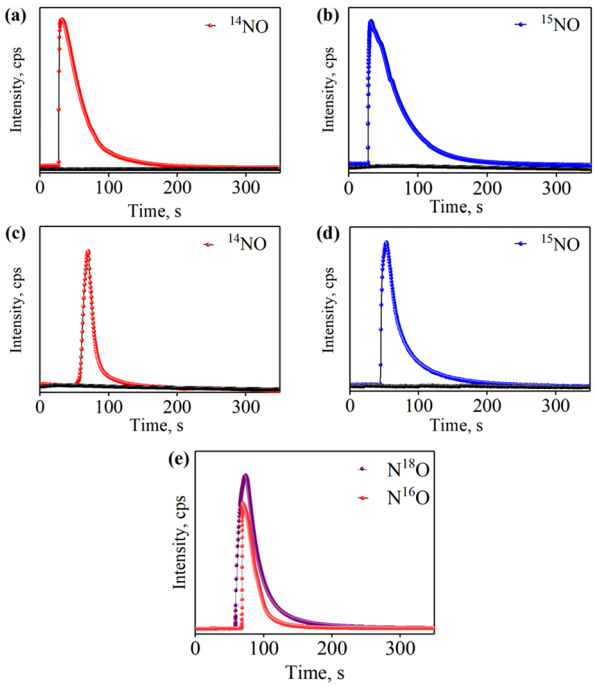

Fig. 4 The time-dependence plots of the formation of (a) ^{14}NO in the reaction of **1**-$^{14}NO_2^-$ (5.0 mM) with one equivalent of H^+ (5.0 mM), (b) ^{15}NO in the reaction of **1**-$^{15}NO_2^-$ (5.0 mM) with one equivalent of H^+ (5.0 mM), (c) ^{14}NO in the reaction of **1**-$^{14}NO_2^-$ (5.0 mM) with two equivalents of H^+ (5.0 mM), (d) ^{15}NO in the reaction of **1**-$^{15}NO_2^-$ (5.0 mM) with two equivalents of H^+ (5.0 mM) and (e) $N^{18}O$ (purple) and $N^{16}O$ (red) in the reaction of **1**-$^{18}ONO^-$ (5.0 mM) with one equivalent of H^+ (5.0 mM), as monitored by the gas-mass analyzer.

nitrosyl stretching at 1704 cm^{-1} $\{Co^{14}NO\}^8$, and this peak shifted to 1674 cm^{-1} when $\{Co^{15}NO\}^8$ was prepared by reacting ^{15}N-labeled-nitrite (Cu^{II}-$^{15}NO_2^-$) with H^+ (ES and ESI, Fig. S7a, b†).[25,38] The shift of NO stretching (Δ = 30 cm^{-1}) indicates that the N atom in the nitrosyl ligand is derived from Cu^{II}-$^{14/15}NO_2^-$. In addition to FT-IR, we investigated the $NO_{(g)}$ derived from the reaction of Cu^{II}-$^{15}NO_2^-$ with H^+ by ESI-MS. The mass spectrum of $\{CoNO\}^8$ showed a prominent peak at *m*/*z* 404.2, $[(12\text{-TMC})Co(^{14}NO)(BF_4)]^+$ (calcd *m*/*z* 404.2), which changed to 405.2 $[(12\text{-TMC})Co(^{15}NO)(BF_4)]^+$ (calcd *m*/*z* 405.2) when the reaction was executed using Cu^{II}-$^{15}NO_2^-$ (ES and ESI, Fig. S7c, d†), indicating clearly that NO in $\{CoNO\}^8$ is derived from the NO_2^- moiety of **1**. Further, to compute the $NO_{(g)}$ formed in the H^+-catalysed reaction of the Cu^{II}-bound NO_2^- moiety, we quantified the amount of $\{CoNO\}^8$ (90 ± 5% with one equivalent of H^+ and 85 ± 5% with two equivalents of H^+) generated in the above reaction by comparing its molar extinction coefficient (ε) value at 370 nm with the authentic $\{CoNO\}^8$ sample (ES and ESI, Fig. S8†).[18a,b]

Mechanistic investigation of the reaction of NO_2^- with H^+ at the Cu^{II}-center

The above findings show how the different equivalents of H^+ lead to $NO_{(g)}$ generation with two diverse side products. This is in contrast to the reports on H^+-induced NO_2^- reduction chem-

istry and biomimetic modeling of the NiR system, where N–O bond breaking in the ON–OH moiety generates $NO_{(g)}$ along with H_2O (using $2H^+ + e^-$).[34b,39] It has also been observed that H^+-induced NO_2^- reduction generates NO along with a metal hydroxide[27a,40] or H_2O_2 ($^{\bullet}OH$)[25,26] and is accomplished *via* the proposed ONOH intermediate similar to that reported for Cu-NiR chemistry.[41] A Cu(ONOH) intermediate has also been proposed in the H^+-induced NO_2^- reduction reaction at the Cu^I center[27b] and established theoretically by Shigeta *et al.*[42] & Chen and co-workers.[22] Hence, we believe that the proposed $[Cu\text{-}ONOH]^{2+}$ intermediate is formed in the reaction of **1** with different amounts of H^+ and generating $NO_{(g)}$ with different side products. Based on the above results, we propose here that the 1st step of the reaction is the electrophilic addition of H^+ to $Cu^{II}\text{-}NO_2^-$, which generates the proposed transient $[Cu\text{-}ONOH]^{2+}$ intermediate (Scheme 2, reaction I). By following the mechanism suggested for $[M\text{-}(ONOH)]^{n+}$ generation,[25,27b,43] the proposed $[Cu\text{-}ONOH]^{2+}$ intermediate leads to the formation of $NO_{(g)}$ and H_2O_2 ($^{\bullet}OH$)[25,26] *via* the homolytic cleavage of the ON-OH moiety (Scheme 2, reaction II).[19,44] The formed H_2O_2 further undergoes a disproportion reaction to form H_2O.[31] However, the sequence of the NO_2^- reaction in the presence of ≈two equivalents of H^+ is believed to proceed *via* the formation of the proposed $[Cu\text{-}ONOH]^{2+}$[25,27b,43] species (Scheme 2, reaction III). The proposed $[Cu\text{-}ONOH]^{2+}$ intermediate may generate $NO_{(g)}$ and H_2O by the decomposition of H_2O_2 in the presence of another H^+, as reported for the H^+-catalysed transformation of H_2O_2 to H_2O.[30,32] Moreover, the metal center (Cu^{II}) plays a crucial role in the selective production of $NO_{(g)}$ as a major product along with H_2O_2 in the reaction of **1** with one equivalent of H^+, while, on the other hand, the reaction of NO_2^- (without Cu^{II}) with H^+ or HONO (without metal) independently decomposes and generates an equimolar amount of NO, NO_2 and H_2O.[45]

Spectroscopic determination and quantification of H_2O_2 and H_2O

To validate our proposed NO_2^- reaction sequences of at the Cu^{II} center, we reacted **1** with varying amounts of $HClO_4$ (H^+ ion source) and spectroscopically determined the formation of different side products. We characterized and followed H_2O_2 and H_2O formation with time by ^{1}H-NMR spectroscopic measurements.[46] The ^{1}H-NMR spectrum of **1** with one equivalent of H^+ in CD_3CN showed a characteristic signal for H_2O_2 (8.66 ppm, Fig. S9a†). Comparison of this spectrum with the authentic samples (i) H_2O_2 plus **3** (8.66 ppm; Fig. S9b†) and (ii) H_2O_2 only (8.66 ppm; Fig. S9c†) validated our theory of H_2O_2 formation in the reaction of **1** with H^+, as observed in our previous report.[25] Further, when labeled Cu^{II} NO_2^- (**1**-$^{18}ONO^-$) was reacted with one equivalent of H^+, we observed a signal at 8.66 ppm in the ^{1}H-NMR spectrum, again confirming that the NO_2^- ligand is the source of hydrogen peroxide (Fig. S9f†). In addition, we followed the generation of H_2O_2 *via* ^{1}H-NMR. We found that the intensity of the H_2O_2 peak (at 8.66 ppm) increased with time and started decreasing after complete formation (Fig. 5a), which is believed to indicate the natural decomposition of H_2O_2 to H_2O with time (Fig. 5b).[31a] Furthermore, ^{1}H-NMR spectral quantification of H_2O_2 using benzene as an internal standard suggested that more than 30% H_2O_2 with respect to **1** was formed in the reaction (ES and ESI, Fig. S9†).[46] In addition to ^{1}H-NMR, we quantified H_2O_2 formation by iodometric titration in the presence of one equivalent of H^+ and found it to be ~31% (ES and ESI, Fig. S10†). We also characterized the generation of H_2O in the reaction of **1** with two equivalents of H^+ by ^{1}H-NMR spectroscopy (ES and ESI, Fig. S11†). The ^{1}H-NMR of the reaction mixture of **1** with two equivalents of H^+ showed a peak for the H_2O protons (2.2 ppm, Fig. S12a†), while the same reaction in

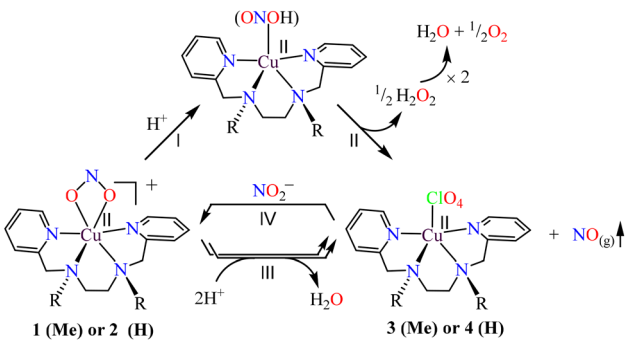

Scheme 2

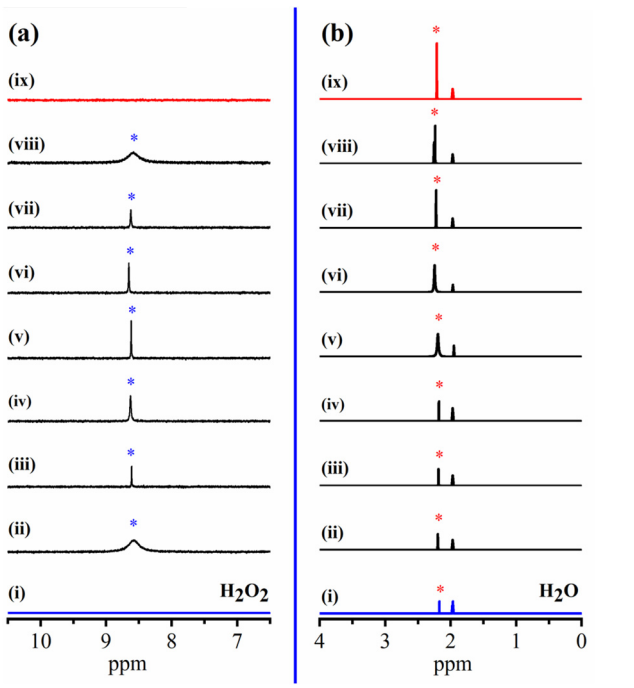

Fig. 5 The ^{1}H-NMR spectra of (a) H_2O_2 (blue asterisk) and (b) H_2O (red asterisk) formation in the reaction of **1** with one equivalent of H^+ recorded at different times in CD_3CN (the blue line indicates **1** before the addition of H^+, and the red line shows the product after the reaction of **1** with one equivalent of H^+).

the presence of D^+ did not show this peak as the final product was D_2O (Fig. S12b†). However, we could not quantify H_2O generation but scientifically established the mechanistic aspect of the H^+-catalyzed conversion of NO_2^- to $NO_{(g)}$ in the presence of the different amounts of H^+. These real-time tracking experiments of H_2O_2/H_2O formation in the reaction of Cu^{II}-NO_2^- with different amounts of acids (or H^+ ions) present new results.

Trapping of the [Cu-ONOH]$^{2+}$ intermediate using 2,4-di-*tert* butyl-phenol

Previous studies on H^+-induced NO_2^- reduction and biomimetic modeling of NiR chemistry suggest the presence of a metal-nitrous acid intermediate before NO generation. Such intermediate species are known to be highly unstable; thus, our attempt to spectroscopically characterize the intermediate species was futile. Hence, we gathered more evidence for our proposed mechanistic reaction sequences by tracking the N–O bond breaking of the proposed [Cu-ONOH]$^{2+}$ intermediate, H_2O_2 ($^{\bullet}$OH radical) generation and H_2O formation. As per the reports and our previous report on ON–OH homolysis,[25] we performed $^{\bullet}$OH radical-trapping experiments using 2,4-di-*tert* butyl-phenol (2,4-DTBP).[43,44] In the reaction of **1** with one equivalent of H^+, we observed the formation of 3,5-Di-*tert*-butylcatechol (3,5-DTBC, ~20%) and 2,4-DTBP-dimer (2,4-DTBP-D, ~10%) with nitro-2,4-DTBP (NO_2-2,4-DTBP, ~4%) (ES and ESI, Fig. S13†). However, negligible amounts of these transformed products of 2,4-DTBP were obtained when the reaction was performed with two equivalents of H^+, suggesting the conversion of H_2O_2 ($^{\bullet}$OH) to H_2O.[25,30a,31a] The above experiments undoubtedly confirm the reaction sequence that N–O bond homolysis forms $^{\bullet}$OH free radicals from the ON–OH moiety, generating different products (Scheme 3), and hence indirectly proves the formation of the [Cu-(ONOH)]$^{2+}$ intermediate in the reaction of **1** with one equivalent of H^+.

As reported in our previous report, the transformation of 2,4-DTBP in the presence of one equivalent of H^+ can be explained based on a radical coupling reaction.[25] First, H-atom abstraction from DTBP by the [Cu-ONOH]$^{2+}$ species generates a phenoxyl radical along with $NO_{(g)}$ and the initial Cu^{II}-complex (Scheme 3, reactions I and II). The phenoxyl radical dimerizes to give 2,4-DTBP-D (Scheme 3, reaction III) or reacts with another molecule of [Cu-ONOH]$^{2+}$ to generate 3,5-DTBC with the release of $NO_{(g)}$ (Scheme 3, reaction IV). Likewise, it may produce NO_2-DTBP in the presence of two molecules of [Cu-ONOH]$^{2+}$ (Scheme 3, reaction V). In addition, we observed the formation of 3,5-DTBC-OH(OD) (223.1) in the reaction of **1** with $DClO_4$ (D^+) in the presence of 2,4-DTBP (ES and ESI, Fig. S13d†). Therefore, the $^{\bullet}$OH radical-induced transformation products support the proposed reaction mechanism, which involves $NO_{(g)}$ generation along with H_2O_2 *via* homolytic N–O bond cleavage in the [Cu-ONOH]$^{2+}$ intermediate species. Moreover, to prove the formation of H_2O_2 in the above reaction, we carried out the reaction of **1**-$^{18}ONO^-$ with one equivalent of H^+ in the presence of 2,4-DTBP. In this reaction, we observed the generation of an intense peak corresponding to 3,5-DTBC-$^{18}OH^{16}OH$ (calc. = 224.1) and 3,5-DTBC-$^{16}OH^{16}OH$ (222.1) in GC-MS (ES and ESI, Fig. S14†). A shift of 3,5-DTBC mass by two-unit values establishes that NO_2^- is the source of the $^{\bullet}$OH radical formed in the reaction and also indirectly authorizes that H_2O_2 is derived from the NO_2^- ligand. Furthermore, we used thioanisole to trap the formed H_2O_2, and the formation of the oxidized product methyl phenyl sulfoxide confirms peroxide formation in the reaction (ES and ESI, Fig. S15†).[47]

Acid-catalyzed conversion of NO_2^- to $NO_{(g)}$ at Cu^{II}-center

To establish catalytic $NO_{(g)}$ generation from **1** in the presence of H^+ ions, we reacted **3** (obtained in the first cycle) with one equivalent of $NaNO_2$ to regenerate **1** and calculated its yield by comparing the absorption at 375 nm, and it was found to be 98% with respect to the authentic sample (Fig. 6, ES and ESI, Fig. S16†). After that, we reacted the formed **1** with the acid to generate $NO_{(g)}$ and **3**; further, after purging with Ar, we reacted **3** with one-equivalent $NaNO_2$ to generate **1** and calculated its % yield by comparing the absorbance at 375 nm. We then repeated several cycles of $NO_{(g)}$ formation from the reaction of

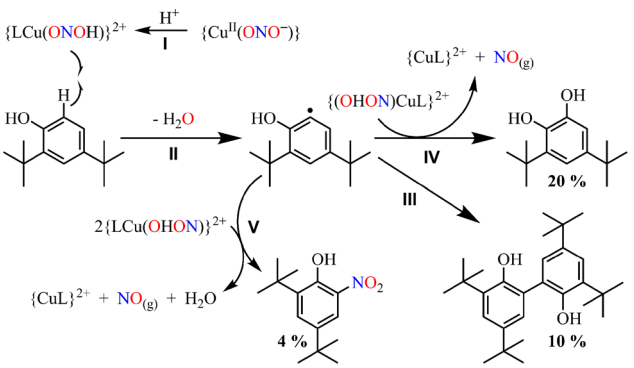

Scheme 3

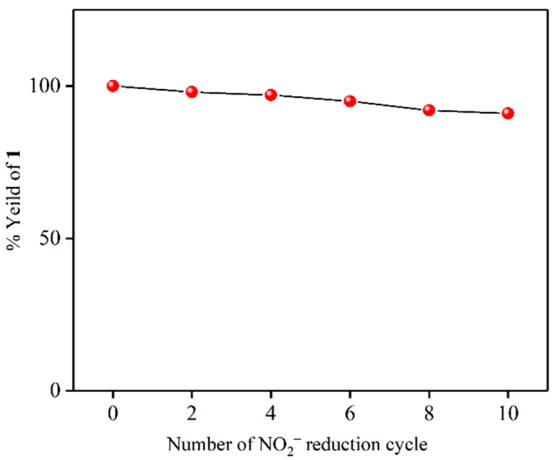

Fig. 6 The percentage yield of **1** formed after 2, 4, 6, 8, and 10 cycles of the reaction of **1** with H^+ ions followed by the addition of one-equivalent $NaNO_2$.

1 with H^+. The Cu^{II} centre could be regenerated and produced **1** from **3** up to ≈95% (after the H^+-catalyzed conversion of NO_2^- to $NO_{(g)}$ at the Cu^{II} center) upon reaction with NO_2^- even after 10 cycles of catalytic reactivity, undoubtedly establishing that Cu^{II} in **1** catalyzes the conversion of NO_2^- to $NO_{(g)}$ in the presence of H^+ ions.

The reaction of $[(H_2BPMEN)Cu^{II}(NO_2^-)]^+$ (2) with acid

Additionally, to obtain additional pieces of evidence for $NO_{(g)}$ generation and to determine the effect of the ligand frameworks, we reacted another Cu^{II}-NO_2^- complex (**2**) with different amounts of H^+ (one or two equivalents). Upon reaction with one-equivalent H^+, we observed a direct change in the characteristic UV-vis band of **2** and the formation of a new band corresponding to **4**, also conforming with the other spectral measurements (Fig. 7a & b, ES & ESI, Fig. S17†) regarding $NO_{(g)}$ formation (Fig. 7c). Similar UV-vis spectral changes were observed when we reacted **2** with two equivalents of H^+, and the product analysis confirmed the generation of **4** (ES & ESI, Fig. S18†), and the gas mass analyzer showed a high-intensity peak for $NO_{(g)}$ (Fig. 7d). In addition to $NO_{(g)}$, we observed other side products, *viz.* H_2O_2 and H_2O, with one- and two-equivalent H^+, respectively (ESI, Fig. S19†). Further, we trapped $NO_{(g)}$ using $[(12\text{-TMC})Co^{II}(NCCH_3)]^{2+}$, which led to the generation of $\{CoNO\}^8$, confirming $NO_{(g)}$ generation in the above reactions (ES, ESI, Fig. S20†).[25,38] In addition to exploring the effect of the electron-donating group (methyl) on the N-atom of the ligand framework, we explored the kinetic measurements. These measurements suggested that the second-order rate constant (k_2) of NO_2^- conversion to $NO_{(g)}$ in the case of **1** was 1.1 times that of **2** (ESI, Fig. S21†). This indicates that the high electron density due to the methyl group on the Cu center supports faster conversion of NO_2^- to $NO_{(g)}$, which can also be correlated with the binding constants (k_b) of NO_2^- with the Cu centers in **1** and **2** (**2**-k_b > **1**-k_b) (ESI, Fig. S22†). In addition, we observed a similar acid-catalyzed NO_2^- to $NO_{(g)}$ conversion cycle on the Cu^{II} center of **2**, as observed for **1**.

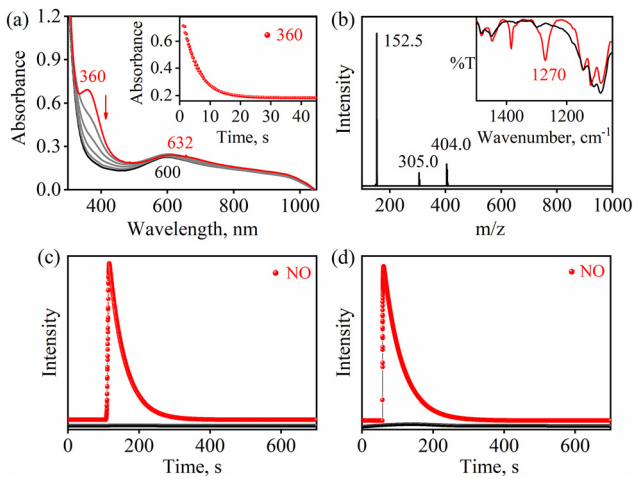

Fig. 7 The UV-vis spectral changes of **2** (1 mM, red line) upon the addition of one equivalent of H^+ under Ar in CH_3CN at 298 K. Inset: the time course of the reaction of **2** monitored at 360 nm (red circles) upon the addition of one equivalent of H^+. (b) The ESI-MS spectrum of **4**. The peak at 152.5 and 404.0 are assigned to $[(H_2BPMEN)Cu]^{2+}$ (calcd *m*/*z* 152.5) and $[(H_2BPMEN)Cu(ClO_4)]^+$ (calcd *m*/*z* 404.0), respectively. Inset: the FT-IR spectra of **2** (red line) and **4** (black line) in KBr. The time-dependent formation of (c) ^{14}NO (red circles) in the reaction of **2**-$^{14}NO_2^-$ (5.0 mM) with one equivalent of H^+ and (d) ^{14}NO (red circles) in the reaction of **2**-$^{14}NO_2^-$ (5.0 mM) with two equivalents of H^+, as monitored by the gas-mass analyzer.

Conclusion

Acid (H^+)-induced conversion of NO_2^- to NO is one of the key research areas concerning biomedical science,[3] industrial applications,[48] and the involvement of reduced product (NO) in various biological reactions.[1d,49] Therefore, understanding the reaction mechanism of NO_2^- to $NO_{(g)}$ conversion in the presence of varying amounts of H^+ (at different pH) and the formation of reaction products in addition to NO[7a,b,9] is very exciting and necessary.[50] In addition, developing a suitable molecular catalyst for the catalytic conversion of NO_2^- to $NO_{(g)}$ is one of the biggest challenges faced by the scientific community. As only a few reports using the electrochemical method are available;[24,28a,b,51] the acid-induced catalytic conversion of NO_2^- to $NO_{(g)}$ is not well-explored. In this report, we have synthesized and spectroscopically characterized two Cu^{II}-nitrito complexes, namely $[(Me_2BPMEN)Cu^{II}(NO_2^-)]^+$ (**1**) and $[(H_2BPMEN)Cu^{II}(NO_2^-)]^+$ (**2**), and established their reactions with different ratios of acid (H^+ ions donor) to develop a molecular catalyst $NO_{(g)}$ formation. Herein, we have shown the disproportionation/conversion of NO_2^- to $NO_{(g)}$ at the Cu^{II} center, and the generation of H_2O_2 or H_2O with $NO_{(g)}$ in the reaction of **1** (or **2**) with one- or ~two-equivalent H^+ ($HClO_4$, a H^+ ion source). We observed the catalytic generation of $NO_{(g)}$ (10 cycles) from the reaction of the Cu^{II} center of **1** (or **2**) with H^+. We followed and investigated NO_2^- transformation at the Cu^{II} center using ^{15}N-labeled-$^{15}NO_2^-$ and ^{18}O-labeled-$^{16}O^{14}N^{18}O^-$, which revealed that the N-atom and O-atom of $NO_{(g)}$ are derived from $^{15}NO_2^-$ and the $^{16}O^{14}N^{18}O^-$ ligand, as confirmed by the observation of $^{15}NO_{(g)}$ and $N^{18}O_{(g)}$ in the headspace gas chromatography/mass spectra, respectively. Further, the side product of NO_2^- conversion to $NO_{(g)}$ was found to be H_2O_2 when **1** (or **2**) was reacted with one-equivalent H^+. Surprisingly, we observed the formation of H_2O when **1** (or **2**) reacted with two-equivalent H^+. The formation of H_2O_2 and H_2O was further detected using ^1H-NMR spectroscopy. Based on the previous examples of H^+-induced NO_2^- reduction reactions and NiR enzymatic reactions,[19,27b,41,42] which propose the formation of a metal-ONOH intermediate before NO generation, the H^+-induced NO_2^- reaction at the Cu^{II} center in **1** (or **2**) is believed to form **3** (or **4**) *via* the formation of a putative $[Cu(ONOH)]^{2+}$ intermediate, which upon disproportionation generates $NO_{(g)}$. The N–O bond homolysis of the proposed ON-OH intermediate is supported by $^{\bullet}OH$ trapping reactions conducted using 2,4-DTBP in the reaction of **1**-$ON^{16}O^-$ ($^{16}ON^{18}O^-$) with one-equivalent H^+. Additionally, the obser-

vation of DTBC(OD) in the reaction of **1** with D^+ further supports the N–O bond homolysis of the proposed ONOH intermediate. Finally, the detection of a significant amount of H_2O_2 (^{1}H-NMR and UV-vis iodometric titration)[46] along with $NO_{(g)}$ release verifies our proposed mechanism.[17] The potential pathway of H_2O formation in the NO_2^- reaction at the Cu^{II}-center with two-equivalent H^+ is *via* the H^+-induced disproportionation/decomposition of H_2O_2 to H_2O. In addition to the mechanistic pathway, we observed a recovery of ~90% of the initial Cu^{II}-NO_2^- complex after more than 10 catalytic cycles of NO_2^- to $NO_{(g)}$ conversion. The present study reports H^+-catalyzed NO_2^- disproportionation to form $NO_{(g)}$ at Cu^{II} centers with different amounts of H^+, showing H_2O_2 and/or H_2O formation by a possible homolytic cleavage of ON–OH.[52] These results add an entirely new mechanistic insight and propose systematic reaction sequences for H^+-induced catalytic NO_2^- disproportionation/conversion reactions, besides explaining why $NO_{(g)}$ and H_2O are formed as end products in NO_2^- reduction reactions at high H^+ concentrations.[50,53]

Conflicts of interest

There are no conflicts to declare.

Acknowledgements

This work was supported by Grants-in-Aid (CRG/2021/003371) from SERB-DST. P. B. Kulbir, thank IISER Tirupati for their fellowship.

References

1 (*a*) R. F. Furchgott, Endothelium–Derived Relaxing Factor: Discovery, Early Studies, and Identification as Nitric Oxide, *Angew. Chem., Int. Ed.*, 1999, **38**, 1870–1880; (*b*) L. J. Ignarro, Nitric Oxide: A Unique Endogenous Signaling Molecule in Vascular Biology, *Angew. Chem., Int. Ed.*, 1999, **38**, 1882–1892; (*c*) L. J. Ignarro, *Nitric Oxide: Biology and Pathobiology*, Academic press, 2000; (*d*) G. B. Richter-Addo, P. Legzdins and J. Burstyn, Introduction: nitric oxide chemistry, *Chem. Rev.*, 2002, **102**, 857–860; (*e*) I. M. Wasser, S. de Vries, P. Moënne-Loccoz, I. Schröder and K. D. Karlin, Nitric Oxide in Biological Denitrification: Fe/Cu Metalloenzyme and Metal Complex NOx Redox Chemistry, *Chem. Rev.*, 2002, **102**, 1201–1234; (*f*) N. Lehnert, E. Kim, H. T. Dong, J. B. Harland, A. P. Hunt, E. C. Manickas, K. M. Oakley, J. Pham, G. C. Reed and V. S. Alfaro, The Biologically Relevant Coordination Chemistry of Iron and Nitric Oxide: Electronic Structure and Reactivity, *Chem. Rev.*, 2021, **121**, 14682–14905.

2 R. B. S. Nabi, R. Tayade, A. Hussain, K. P. Kulkarni, Q. M. Imran, B.-G. Mun and B.-W. Yun, Nitric oxide regulates plant responses to drought, salinity, and heavy metal stress, *Environ. Exp. Bot.*, 2019, **161**, 120–133.

3 F. Vargas, J. M. Moreno, R. Wangensteen, I. Rodriguez-Gomez and J. Garcia-Estan, The Endocrine System in Chronic Nitric Oxide Deficiency, *Eur. J. Endocrinol.*, 2007, **156**, 1–12.

4 (*a*) R. E. Huie and S. Padmaja, The Reaction of no With Superoxide, *Free Radical Res. Commun.*, 1993, **18**, 195–199; (*b*) P. Pacher, J. S. Beckman and L. Liaudet, Nitric oxide and peroxynitrite in health and disease, *Physiol. Rev.*, 2007, **87**, 315–424; (*c*) C. Prolo, M. N. Alvarez and R. Radi, Peroxynitrite, a Potent Macrophage-derived Oxidizing Cytotoxin to Combat Invading Pathogens, *BioFactors*, 2014, **40**, 215–225.

5 (*a*) W. C. Nottingham and J. R. Sutter, Kinetics of the Oxidation of Nitric Oxide by Chlorine and Oxygen in Nonaqueous Media, *Int. J. Chem. Kinet.*, 1986, **18**, 1289–1302; (*b*) C. H. Lim, P. C. Dedon and W. M. Deen, Kinetic analysis of intracellular concentrations of reactive nitrogen species, *Chem. Res. Toxicol.*, 2008, **21**, 2134–2147.

6 (*a*) R. Radi, Nitric Oxide, Oxidants, and Protein Tyrosine Nitration, *Proc. Natl. Acad. Sci. U. S. A.*, 2004, **101**, 4003–4008; (*b*) B. Kalyanaraman, Nitrated Lipids: A Class of Cell-Signaling Molecules, *Proc. Natl. Acad. Sci. U. S. A.*, 2004, **101**, 11527–11528; (*c*) P. C. Dedon and S. R. Tannenbaum, Reactive nitrogen species in the chemical biology of inflammation, *Arch. Biochem. Biophys.*, 2004, **423**, 12–22.

7 (*a*) B. A. Averill, Dissimilatory Nitrite and Nitric Oxide Reductases, *Chem. Rev.*, 1996, **96**, 2951–2964; (*b*) E. I. Tocheva, F. I. Rosell, A. G. Mauk and M. E. Murphy, Side-on copper-nitrosyl coordination by nitrite reductase, *Science*, 2004, **304**, 867–870; (*c*) N. Lehnert, T. C. Berto, M. G. I. Galinato and L. E. Goodrich, in *Handbook of Porphyrin Science*, ed. K. Kadish, K. Smith and R. Guilard, World Scientific Publishing, Singapore, 2011, pp. 1.

8 (*a*) T. B. McCall, N. K. Boughton-Smith, R. M. Palmer, B. J. Whittle and S. Moncada, Synthesis of Nitric Oxide from L-arginine by Neutrophils. Release and Interaction with Superoxide Anion, *Biochem. J.*, 1989, **261**, 293–296; (*b*) R. G. Knowles and S. Moncada, Nitric Oxide Synthases in Mammals, *Biochem. J.*, 1994, **298**(Pt 2), 249–258.

9 T. S. Kurtikyan, A. A. Hovhannisyan, A. V. Iretskii and P. C. Ford, Six-coordinate nitro complexes of iron(III) porphyrins with trans S-donor ligands. Oxo-transfer reactivity in the solid state, *Inorg. Chem.*, 2009, **48**, 11236–11241.

10 (*a*) B. C. Sanders, S. M. Hassan and T. C. Harrop, NO2(-) activation and reduction to NO by a nonheme Fe(NO2)2 complex, *J. Am. Chem. Soc.*, 2014, **136**, 10230–10233; (*b*) S. Kundu, W. Y. Kim, J. A. Bertke and T. H. Warren, Copper(II) Activation of Nitrite: Nitrosation of Nucleophiles and Generation of NO by Thiols, *J. Am. Chem. Soc.*, 2017, **139**, 1045–1048.

11 (*a*) A. K. Patra, R. K. Afshar, J. M. Rowland, M. M. Olmstead and P. K. Mascharak, Thermally induced stoichiometric and catalytic O-atom transfer by a non-heme iron(III)-nitro complex: first example of reversible [Fe-NO]7<-->FeIII-NO2

transformation in the presence of dioxygen, *Angew. Chem., Int. Ed.*, 2003, **42**, 4517–4521; (*b*) L. Cheng, D. R. Powell, M. A. Khan and G. B. Richter-Addo, The first unambiguous determination of a nitrosyl-to-nitrite conversion in an iron nitrosyl porphyrin, *Chem. Commun.*, 2000, 2301–2302, DOI: 10.1039/B006775J.

12 S. Hong, J. J. Yan, D. G. Karmalkar, K. D. Sutherlin, J. Kim, Y. M. Lee, Y. Goo, P. K. Mascharak, B. Hedman, K. O. Hodgson, K. D. Karlin, E. I. Solomon and W. Nam, A mononuclear nonheme {FeNO}(6) complex: synthesis and structural and spectroscopic characterization, *Chem. Sci.*, 2018, **9**, 6952–6960.

13 (*a*) S. Hematian, M. A. Siegler and K. D. Karlin, Heme/copper assembly mediated nitrite and nitric oxide interconversion, *J. Am. Chem. Soc.*, 2012, **134**, 18912–18915; (*b*) S. Hematian, I. Kenkel, T. E. Shubina, M. Dürr, J. J. Liu, M. A. Siegler, I. Ivanovic-Burmazovic and K. D. Karlin, Nitrogen Oxide Atom-Transfer Redox Chemistry; Mechanism of NO(g) to Nitrite Conversion Utilizing μ-oxo Heme-FeIII–O–CuII(L) Constructs, *J. Am. Chem. Soc.*, 2015, **137**, 6602–6615.

14 J. Brooks and D. Keilin, The action of nitrite on haemoglobin in the absence of oxygen, *Proc. R. Soc. London, Ser. B*, 1937, **123**, 368–382.

15 J. Heinecke and P. C. Ford, Mechanistic Studies of Nitrite Reactions with Metalloproteins and Models Relevant to Mammalian Physiology, *Coord. Chem. Rev.*, 2010, **254**, 235–247.

16 (*a*) A. P. Hunt and N. Lehnert, Heme-nitrosyls: Electronic Structure Implications for Function in Biology, *Acc. Chem. Res.*, 2015, **48**, 2117–2125; (*b*) A. L. Speelman, B. Zhang, C. Krebs and N. Lehnert, Structural and Spectroscopic Characterization of a High-Spin $\{FeNO\}^6$ Complex with an Iron(IV)–NO– Electronic Structure, *Angew. Chem., Int. Ed.*, 2016, **55**, 6685–6688.

17 A. M. Wright, G. Wu and T. W. Hayton, Structural Characterization of a Copper Nitrosyl Complex with a $\{CuNO\}^{10}$ Configuration, *J. Am. Chem. Soc.*, 2010, **132**, 14336–14337.

18 (*a*) P. Kumar, Y. M. Lee, Y. J. Park, M. A. Siegler, K. D. Karlin and W. Nam, Reactions of Co(III)-nitrosyl Complexes with Superoxide and Their Mechanistic Insights, *J. Am. Chem. Soc.*, 2015, **137**, 4284–4287; (*b*) P. Kumar, Y. M. Lee, L. Hu, J. Chen, Y. J. Park, J. Yao, H. Chen, K. D. Karlin and W. Nam, Factors That Control the Reactivity of Cobalt(III)–Nitrosyl Complexes in Nitric Oxide Transfer and Dioxygenation Reactions: A Combined Experimental and Theoretical Investigation, *J. Am. Chem. Soc.*, 2016, **138**, 7753–7762; (*c*) S. Hong, J. J. Yan, D. G. Karmalkar, K. D. Sutherlin, J. Kim, Y. M. Lee, Y. Goo, P. K. Mascharak, B. Hedman, K. O. Hodgson, K. D. Karlin, E. I. Solomon and W. Nam, A Mononuclear Nonheme $\{FeNO\}^6$ Complex: Synthesis and Structural and Spectroscopic Characterization, *Chem. Sci.*, 2018, **9**, 6952–6960.

19 W. M. Ching, P. P. Chen and C. H. Hung, A mechanistic study of nitrite reduction on iron(II) complexes of methylated N-confused porphyrins, *Dalton Trans.*, 2017, **46**, 15087–15094.

20 (*a*) J. L. Heinecke, C. Khin, J. C. Pereira, S. A. Suarez, A. V. Iretskii, F. Doctorovich and P. C. Ford, Nitrite Reduction Mediated by Heme Models. Routes to NO and HNO?, *J. Am. Chem. Soc.*, 2013, **135**, 4007–4017; (*b*) T. S. Kurtikyan, A. A. Hovhannisyan and P. C. Ford, Six-Coordinate Ferrous Nitrosyl Complex Fe(II)(TTP)(PMe_3)(NO) (TTP = meso-Tetra-p-tolylporphyrinato Dianion), *Inorg. Chem.*, 2016, **55**, 9517–9520.

21 M. Kumar, N. A. Dixon, A. C. Merkle, M. Zeller, N. Lehnert and E. T. Papish, Hydrotris(triazolyl)borate complexes as functional models for Cu nitrite reductase: the electronic influence of distal nitrogens, *Inorg. Chem.*, 2012, **51**, 7004–7006.

22 S. C. Hsu, Y. L. Chang, W. J. Chuang, H. Y. Chen, I. J. Lin, M. Y. Chiang, C. L. Kao and H. Y. Chen, Copper(I) nitro complex with an anionic [HB(3,5-Me2Pz)3]- ligand: a synthetic model for the copper nitrite reductase active site, *Inorg. Chem.*, 2012, **51**, 9297–9308.

23 R. C. Maji, S. K. Barman, S. Roy, S. K. Chatterjee, F. L. Bowles, M. M. Olmstead and A. K. Patra, Copper complexes relevant to the catalytic cycle of copper nitrite reductase: electrochemical detection of NO(g) evolution and flipping of NO2 binding mode upon Cu(II) –> Cu(I) reduction, *Inorg. Chem.*, 2013, **52**, 11084–11095.

24 C. J. White, J. M. Schwartz, N. Lehnert and M. E. Meyerhoff, Reducing O2 Sensitivity in Electrochemical Nitric Oxide Releasing Catheters: An O2-Tolerant Copper(II)-Ligand Nitrite Reduction Catalyst and a Glucose Oxidase Catheter Coating, *Bioelectrochemistry*, 2023, 108448.

25 M. A. Puthiyaveetil Yoosaf, S. Ghosh, Y. Narayan, M. Yadav, S. C. Sahoo and P. Kumar, Finding a new pathway for acid-induced nitrite reduction reaction: formation of nitric oxide with hydrogen peroxide, *Dalton Trans.*, 2019, **48**, 13916–13920.

26 Kulbir, S. Das, T. Devi, S. Ghosh, S. Chandra Sahoo and P. Kumar, Acid-induced nitrite reduction of nonheme iron (ii)-nitrite: mimicking biological Fe–NiR reactions, *Chem. Sci.*, 2023, **14**, 2935–2942.

27 (*a*) C. C. Tsou, W. L. Yang and W. F. Liaw, Nitrite activation to nitric oxide via one-fold protonation of iron(II)-O,O-nitrito complex: relevance to the nitrite reductase activity of deoxyhemoglobin and deoxyhemerythrin, *J. Am. Chem. Soc.*, 2013, **135**, 18758–18761; (*b*) M. Kujime and H. Fujii, Spectroscopic characterization of reaction intermediates in a model for copper nitrite reductase, *Angew. Chem., Int. Ed.*, 2006, **45**, 1089–1092.

28 (*a*) A. P. Hunt, A. E. Batka, M. Hosseinzadeh, J. D. Gregory, H. K. Haque, H. Ren, M. E. Meyerhoff and N. Lehnert, Nitric Oxide Generation On Demand for Biomedical Applications via Electrocatalytic Nitrite Reduction by Copper BMPA- and BEPA-Carboxylate Complexes, *ACS Catal.*, 2019, **9**, 7746–7758; (*b*) G. Cioncoloni, I. Roger, P. S. Wheatley, C. Wilson, R. E. Morris, S. Sproules and

M. D. Symes, Proton-Coupled Electron Transfer Enhances the Electrocatalytic Reduction of Nitrite to NO in a Bioinspired Copper Complex, *ACS Catal.*, 2018, **8**, 5070–5084; (*c*) S. E. Braley, H. Y. Kwon, S. Xu, E. Z. Dalton, E. Jakubikova and J. M. Smith, Buffer Assists Electrocatalytic Nitrite Reduction by a Cobalt Macrocycle Complex, *Inorg. Chem.*, 2022, **61**, 12998–13006.

29 Kulbir, S. Das, T. Devi, M. Goswami, M. Yenuganti, P. Bhardwaj, S. Ghosh, S. C. Sahoo and P. Kumar, Oxygen atom transfer promoted nitrate to nitric oxide transformation: a step-wise reduction of nitrate -> nitrite -> nitric oxide, *Chem. Sci.*, 2021, **12**, 10605–10612.

30 (*a*) B. Mlasi, D. Glasser and D. Hildebrandt, Kinetics of the Decomposition of Hydrogen Peroxide in Acidic Copper Sulfate Solutions, *Ind. Eng. Chem. Res.*, 2015, **54**, 5589–5597; (*b*) K. T. Lu, C. C. Yang and P. C. Lin, The criteria of critical runaway and stable temperatures of catalytic decomposition of hydrogen peroxide in the presence of hydrochloric acid, *J. Hazard. Mater.*, 2006, **135**, 319–327.

31 (*a*) P. Pędziwiatr, F. Mikołajczyk, D. Zawadzki, K. Mikołajczyk and A. Bedka, Decomposition of hydrogen peroxide - kinetics and review of chosen catalysts, *Acta Innov.*, 2018, 45–52, DOI: **10.32933/ActaInnovations.26.5**; (*b*) N. Okroj, K. Michalska and B. J. M. W. Jakusz, Effect of vibration and stirring on 90% and 98% hydrogen peroxide, *Mater. Wysokoenerg. / High Energy Mater.*, 2018, **10**, 88–96.

32 (*a*) W. D. Emmons, Peroxytrifluoroacetic Acid. I. The Oxidation of Nitrosamines to Nitramines1, *J. Am. Chem. Soc.*, 1954, **76**, 3468–3470; (*b*) R. S. Livingston and W. C. Bray, The Catalytic Decomposition of Hydrogen Peroxide in an Acid Chlorine-Chloride Solution, *J. Am. Chem. Soc.*, 2002, **47**, 2069–2082.

33 M. Giorgio, M. Trinei, E. Migliaccio and P. G. Pelicci, Hydrogen peroxide: a metabolic by-product or a common mediator of ageing signals?, *Nat. Rev. Mol. Cell Biol.*, 2007, **8**, 722–728.

34 (*a*) F. Cutruzzola, Bacterial nitric oxide synthesis, *Biochim. Biophys. Acta*, 1999, **1411**, 231–249; (*b*) I. M. Wasser, S. de Vries, P. Moenne-Loccoz, I. Schroder and K. D. Karlin, Nitric oxide in biological denitrification: Fe/Cu metalloenzyme and metal complex NOx redox chemistry, *Chem. Rev.*, 2002, **102**, 1201–1234; (*c*) W. G. Zumft, Cell biology and molecular basis of denitrification, *Microbiol. Mol. Biol. Rev.*, 1997, **61**, 533–616.

35 (*a*) T. Pandiyan, H. J. Guadalupe, J. Cruz, S. Bernes, V. M. Ugalde-Salvdivar and I. Gonzalez, DFT and experimental studies of perchlorate ion coordination in cis/trans-copper(II) complexes of tetradentate pyridyl ligands, *Eur. J. Inorg. Chem.*, 2008, **2008**, 3274–3285; (*b*) P. Kumar, A. Kalita and B. Mondal, Nitric oxide reactivity of Cu(II) complexes of tetra- and pentadentate ligands: structural influence in deciding the reduction pathway, *Dalton Trans.*, 2013, **42**, 5731–5739.

36 (*a*) I. M. Procter and F. S. Stephens, An example of a cis-distorted octahedral copper(II) complex: the crystal structure of nitritobis-2,2′-bipyridylcopper(II) nitrate, *J. Chem. Soc. A*, 1969, 1248–1255; (*b*) A. Kalita, P. Kumar, R. C. Deka and B. Mondal, First example of a Cu(I)-(eta2-O,O)nitrite complex derived from Cu(II)-nitrosyl, *Chem. Commun.*, 2012, **48**, 1251–1253.

37 B. A. Averill, Dissimilatory Nitrite and Nitric Oxide Reductases, *Chem. Rev.*, 1996, **96**, 2951–2964.

38 (*a*) P. Kumar, Y. M. Lee, Y. J. Park, M. A. Siegler, K. D. Karlin and W. Nam, Reactions of Co(III)-nitrosyl complexes with superoxide and their mechanistic insights, *J. Am. Chem. Soc.*, 2015, **137**, 4284–4287; (*b*) P. Kumar, Y. M. Lee, L. Hu, J. Chen, Y. J. Park, J. Yao, H. Chen, K. D. Karlin and W. Nam, Factors That Control the Reactivity of Cobalt(III)-Nitrosyl Complexes in Nitric Oxide Transfer and Dioxygenation Reactions: A Combined Experimental and Theoretical Investigation, *J. Am. Chem. Soc.*, 2016, **138**, 7753–7762.

39 L. Casella, O. Carugo, M. Gullotti, S. Doldi and M. Frassoni, Synthesis, Structure, and Reactivity of Model Complexes of Copper Nitrite Reductase, *Inorg. Chem.*, 1996, **35**, 1101–1113.

40 R. Silaghi-Dumitrescu, Linkage Isomerism in Nitrite Reduction by Cytochrome cd1 Nitrite Reductase, *Inorg. Chem.*, 2004, **43**, 3715–3718.

41 S. L. Rose, S. V. Antonyuk, D. Sasaki, K. Yamashita, K. Hirata, G. Ueno, H. Ago, R. R. Eady, T. Tosha, M. Yamamoto and S. S. Hasnain, An unprecedented insight into the catalytic mechanism of copper nitrite reductase from atomic-resolution and damage-free structures, *Sci. Adv.*, 2021, **7**, eabd8523.

42 S. Maekawa, T. Matsui, K. Hirao and Y. Shigeta, Theoretical study on reaction mechanisms of nitrite reduction by copper nitrite complexes: toward understanding and controlling possible mechanisms of copper nitrite reductase, *J. Phys. Chem. B*, 2015, **119**, 5392–5403.

43 S. Suzuki, K. Kataoka and K. Yamaguchi, Metal coordination and mechanism of multicopper nitrite reductase, *Acc. Chem. Res.*, 2000, **33**, 728–735.

44 M. Lintuluoto and J. M. Lintuluoto, Intra-electron transfer induced by protonation in copper-containing nitrite reductase, *Metallomics*, 2018, **10**, 565–578.

45 (*a*) N. Bayliss and D. J. Watts, The decomposition of sodium nitrite solutions in aqueous sulphuric and perchloric acids, *Aust. J. Chem.*, 1963, **16**, 927–932; (*b*) E. W. Kaiser and C. H. Wu, A kinetic study of the gas phase formation and decomposition reactions of nitrous acid, *J. Phys. Chem.*, 1977, **81**, 1701–1706; (*c*) W. H. Chan, R. J. Nordstrom, J. G. Galvert and J. H. Shaw, An IRFTS spectroscopic study of the kinetics and the mechanism of the reactions in the gaseous system, HONO, NO, NO2, H_2O, *Chem. Phys. Lett.*, 1976, **37**, 441–446; (*d*) W. Chan, R. Nordstrom, J. Calvert and J. H. Shaw, Kinetic study of HONO formation and decay reactions in gaseous mixtures of HONO, NO, NO/sub 2/, H/sub 2/O, and N/sub 2, *J. Phys. Chem. A*, 1976, **10**; (*e*) A. Mebel, M.-C. Lin and C. F. Melius, Rate constant of the HONO+ HONO→ H_2O+ NO+ NO2 reac-

tion from ab initio MO and TST calculations, *J. Phys. Chem. A*, 1998, **102**, 1803–1807.

46 N. A. Stephenson and A. T. Bell, Quantitative Analysis of Hydrogen Peroxide by ^{1}H NMR Spectroscopy, *Anal. Bioanal. Chem.*, 2005, **381**, 1289–1293.

47 R. A. Martinez, D. R. Glass, E. G. Ortiz, M. A. Alvarez and C. J. Unkefer, Synthesis of isotopically labeled 1,3-dithiane, *J. Labelled Compd. Radiopharm.*, 2014, **57**, 338–341.

48 M. Marvasi, Potential use and perspectives of nitric oxide donors in agriculture, *J. Sci. Food Agric.*, 2017, **97**, 1065–1072.

49 (*a*) R. F. Furchgott, Endothelium-Derived Relaxing Factor: Discovery, Early Studies, and Identifcation as Nitric Oxide (Nobel Lecture), *Angew. Chem., Int. Ed.*, 1999, **38**, 1870–1880; (*b*) L. J. Ignarro, Nitric oxide: a unique endogenous signaling molecule in vascular biology, *Biosci. Rep.*, 1999, **19**, 51–71.

50 (*a*) Z. H. L. Abraham, B. E. Smith, B. D. Howes, D. J. Lowe and R. R. Eady, pH-dependence for binding a single nitrite ion to each type-2 copper centre in the copper-containing nitrite reductase of Alcaligenes xylosoxidans, *Biochem. J.*, 1997, **324**, 511–516; (*b*) Z. Huang, S. Shiva, D. B. Kim-Shapiro, R. P. Patel, L. A. Ringwood, C. E. Irby, K. T. Huang, C. Ho, N. Hogg, A. N. Schechter and M. T. Gladwin, Enzymatic function of hemoglobin as a nitrite reductase that produces NO under allosteric control, *J. Clin. Invest.*, 2005, **115**, 2099–2107; (*c*) C. A. Clark, C. P. Reddy, H. Xu, K. N. Heck, G. H. Luo, T. P. Senftle and M. S. Wong, Mechanistic Insights into pH-Controlled Nitrite Reduction to Ammonia and Hydrazine over Rhodium, *ACS Catal.*, 2020, **10**, 494–509.

51 S. E. Braley, H.-Y. Kwon, S. Xu, E. Z. Dalton, E. Jakubikova and J. M. Smith, Buffer Assists Electrocatalytic Nitrite Reduction by a Cobalt Macrocycle Complex, *Inorg. Chem.*, 2022, **61**, 12998–13006.

52 S. Suzuki, K. Kataoka and K. Yamaguchi, Metal Coordination and Mechanism of Multicopper Nitrite Reductase, *Acc. Chem. Res.*, 2000, **33**, 728–735.

53 H.-Y. Hu, N. Goto and K. Fujie, Effect of ph on the reduction of nitrite in water by metallic iron, *Water Res.*, 2001, **35**, 2789–2793.